Genome-wide functional analysis of human cell-cycle regulators

Mridul Mukherji*, Russell Bell†, Lubica Supekova*, Yan Wang‡, Anthony P. Orth‡, Serge Batalov‡, Loren Miraglia‡, Dieter Huesken§, Joerg Lange§, Christopher Martin†, Sudhir Sahasrabudhe†, Mischa Reinhardt§, Francois Natt§, Jonathan Hall§, Craig Mickanin¶, Mark Labow¶, Sumit K. Chanda‡, Charles Y. Cho‡‖, and Peter G. Schultz*‡‖

*The Skaggs Institute for Chemical Biology and Department of Chemistry, The Scripps Research Institute, 10550 North Torrey Pines Road, La Jolla, CA 92037; †Prolexys Pharmaceuticals, Inc., 2150 West Dauntless Avenue, Salt Lake City, UT 84116; ‡Genomics Institute of the Novartis Research Foundation, 10675 John Jay Hopkins Drive, San Diego, CA 92121; §Genome and Proteome Sciences, Novartis Institutes for BioMedical Research, CH-4002 Basel, Switzerland; and ¶Genome and Proteome Sciences, Novartis Institutes for BioMedical Research, Inc., 250 Massachusetts Avenue, Cambridge, MA 02139

Contributed by Peter G. Schultz, May 25, 2006

Human cells have evolved complex signaling networks to coordinate the cell cycle. A detailed understanding of the global regulation of this fundamental process requires comprehensive identification of the genes and pathways involved in the various stages of cell-cycle progression. To this end, we report a genome-wide analysis of the human cell cycle, cell size, and proliferation by targeting >95% of the protein-coding genes in the human genome using small interfering RNAs (siRNAs). Analysis of >2 million images, acquired by quantitative fluorescence microscopy, showed that depletion of 1,152 genes strongly affected cell-cycle progression. These genes clustered into eight distinct phenotypic categories based on phase of arrest, nuclear area, and nuclear morphology. Phase-specific networks were built by interrogating knowledge-based and physical interaction databases with identified genes. Genome-wide analysis of cell-cycle regulators revealed a number of kinase, phosphatase, and proteolytic proteins and also suggests that processes thought to regulate G_1-S phase progression like receptor-mediated signaling, nutrient status, and translation also play important roles in the regulation of G_2/M phase transition. Moreover, 15 genes that are integral to TNF/NF-κB signaling were found to regulate G_2/M, a previously unanticipated role for this pathway. These analyses provide systems-level insight into both known and novel genes as well as pathways that regulate cell-cycle progression, a number of which may provide new therapeutic approaches for the treatment of cancer.

high-content screening | network analysis | small interfering RNA | human genome

The eukaryotic cell cycle is a complex process that requires the orderly integration of a myriad of cellular processes for successful completion. Cell growth and metabolism, DNA synthesis, organelle biogenesis, cytoskeletal remodeling, and chromosome segregation all play important roles in multiple phases of the cell cycle. The development of systems-level models that fully describe the cell cycle will require at minimum a comprehensive census of the protein components that are necessary for cell-cycle progression. Classical saturating molecular genetic analyses, mostly in single-cell eukaryotes, have identified many genes with conserved functions in the human cell cycle (1). However, in higher eukaryotes, cell specialization and a plethora of signaling inputs add layers of complexity to cell-cycle analysis.

A promising approach for genome-scale loss-of-function screens is the use of RNA interference (RNAi) by transfection of long double-stranded RNAs, which has been used to study several phenotypes in model organisms such as *Drosophila* and *Caenorhabditis elegans* (2–8), including the cell cycle (9). Because the interferon response in human cells restricts use of this approach, small interfering RNA (siRNA) (10) or short hairpin RNA (shRNA) (11) libraries have been developed to facilitate whole genome studies in human cells. A recent study from the RNAi Consortium described a screen of an arrayed library of 5,000 shRNAs targeting 1,028 genes for regulators of mitosis that identified ≈100 candidate genes; this subset targeted primarily protein kinases, phosphatases, tumor suppressors, and DNA modifying enzymes (12). To identify novel cell-cycle regulators, we have independently depleted 24,373 genes from the human genome with 58,746 synthetic siRNAs and examined genes that alter the cell-cycle distribution of unsynchronized U2OS cells, a well studied osteosarcoma cell line.

Results and Discussion

High-Content Screening of a Genome-Wide siRNA Library. A genome-wide siRNA library targeting 24,373 predicted human genes was designed by using the BIOPREDsi algorithm (10). In addition, 5,000 "druggable" genes, predominantly enzymes and receptors, were targeted with an additional 10,000 siRNAs. After transfection with prespotted arrayed siRNAs in 384-well plates, U2OS cells were grown for 3 days in culture media to allow sufficient time for mRNA depletion and passage through a complete cell cycle (Fig. 1). The cells were fixed, and the nuclei were stained with DAPI to assess cellular DNA content. High-content automated single-cell fluorescence microscopy (13) was used to acquire images covering the complete surface of all wells. Images were shade corrected, background subtracted, and segmented to define discrete objects representing nuclei. Fluorescence intensities, area, and the perimeter-to-area ratio (PAR), a geometric measure of nuclear shape, were calculated for all nuclei. For each well, eight descriptors were computed in terms of standard deviations (σ value) from the plate mean (Fig. 2*A*): total cell number, percentage of cells in G_1, S, and G_2/M phases (determined by gating fluorescence intensities), percentage of cells with 8N DNA content (N, haploid DNA content), the G_1 and G_2/M nuclear areas, and percentage of G_2/M nuclei having high PAR (%G_2/M Hi-PAR). The percentage of G_2/M cells with disproportionately high PAR allowed detection of cytokinetic defects (Figs. 1 and 2*A*). DNA histograms and image segmentations of all genes with high σ for any cell-cycle phase were manually inspected to exclude false positives due to cell clumping. In general, this microscopy-based method of cell-cycle analysis showed excellent agreement with characteristic cell-cycle defects caused by specific small molecules (Fig. 5, which is published as supporting information on the PNAS web site) and with FACS studies after RNAi of selected genes (Fig. 5).

Depletion of 1,152 genes (4.7% of all genes studied) altered cell-cycle progression with high penetrance in two replicates of

Conflict of interest statement: A patent application has been filed for novel cancer drug target genes.

Abbreviations: PAR, perimeter-area ratio; siRNA, small interfering RNA; RNAi, RNA interference; PP1, protein phosphatase 1.

‖To whom correspondence may be addressed. E-mail: ccho@gnf.org or schultz@scripps.edu.

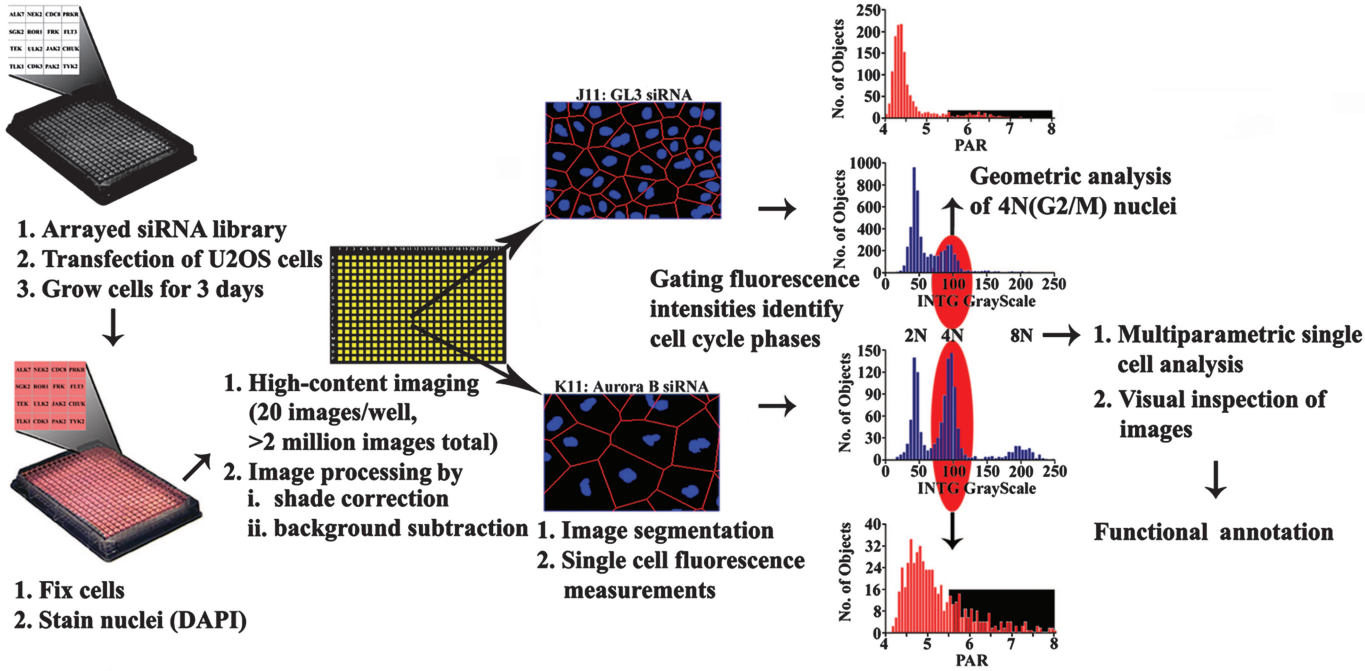

Fig. 1. Scheme for identifying human cell-cycle regulators by RNAi using high-content imaging. Cultured cells were transfected, fixed, stained, and imaged. The percentage of cells in each phase of the cell cycle was determined from processed images. In addition, the percentage of G_2/M cells (red ellipses) with PAR between 5.5 and 8.0 (black rectangles) was calculated for each well. DNA histograms and images for all siRNA wells resulting in significant changes in phase distribution or morphology were manually inspected before functional annotation.

the screen (Table 1, which is published as supporting information on the PNAS web site). We blindly differentiated all positive control wells (e.g., aurora-B siRNA, ≈520 wells) from negative controls spotted during the screen. Previous cell-cycle screens in *Drosophila* have reported low reproducibility (55%) among kinases required in S2 cells (9). Therefore, we verified our results by resynthesizing siRNAs for 57 genes whose cell-cycle phenotypes in this study had not been previously described and confirmed that all of the pooled siRNAs recapitulated the original screen phenotype (Table 2, which is published as supporting information on the PNAS web site). We examined siRNA efficacy in greater detail for a subset of these genes. For 19 of 24 randomly selected genes, at least two independent siRNAs were found that caused the same cell-cycle defects as the pool after testing the original two siRNAs and three additional sequences (Table 2). Reduction in target mRNA levels was observed for 18 of these 19 genes by quantitative RT-PCR (Fig. 6, which is published as supporting information on the PNAS web site).

Comparison of Identified Cell-Cycle Genes with Periodic Expression Data. An important cell-cycle regulatory mechanism is the periodic expression of essential cell-cycle genes. To examine which genes identified in this study show changes in expression levels during the cell cycle, we compared our data with a periodic cell-cycle mRNA expression dataset (14). Among the genes whose loss of function caused severe cell-cycle defects in U2OS cells, 62 had high amplitude during a specific phase of cell cycle in HeLa cells (Table 3, which is published as supporting information on the PNAS web site). Depletion of most of these genes (44/62) caused cell-cycle arrest in the same phase where they had maximum expression. Comparison of the gene expression data with a less stringent list of genes (termed as weak hits, whose depletion resulted in σ values for a phase of ≥ 3 but not reported as a strong hit regulating cell-cycle phase progression in Table 1) from this study identified an additional 108 genes in common. However, knockdown of a lower percentage of the additional genes arrested cells in the phase where their expression peaked (53/108). The limited overlap between the mRNA amplitudes and essential proteins required for cell-cycle progression could be due to "just-in-time" assembly of cell-cycle molecular machines (15), in which the functions of static proteins are controlled by a few dynamic components. Whereas oscillating gene expression patterns are an integral component of cell-cycle control, the particular genes that cycle vary among species. A previous comparison between *Schizosaccharomyces pombe* and *Saccharomyces cerevisiae* expression profiles identified only ≈40 common genes (16). Of these genes, 26 have human orthologs, and we found that depletion of 16 of these caused a cell-cycle defect (Table 3), suggesting these might be evolutionarily conserved core cell-cycle regulatory transcripts.

Identified Cell-Cycle Genes Cluster in Eight Phenotypic Categories. A cluster analysis of these genes produced eight broad categories of cell-cycle defects based on percentage of cells in each phase, nuclear area, and nuclear morphology (Fig. 2*B*). For example, G_1 cells with small nuclear areas (category 1) had reduced cell size and often had condensed α-tubulin and reduced cell numbers, indicating cellular toxicity compared with category 2 genes (G_1 cells with average or larger nuclear area). Depletion of category 3 genes resulted in an increased number of S phase cells, whereas reduction of category 4 genes significantly increased both S and G_2/M phase populations. Down-regulation of category 5 genes resulted in G_2/M cells with large nuclei ($>4\sigma$), whereas G_2/M cells in category 6 were of average or smaller size. Reduction in expression of genes in both categories 7 and 8 resulted in high G_2/M cell number with some polyploidy. The morphology of 4N nuclei of category 7 cells (G_2/M with endoreduplication) was generally similar to that of negative control cells, whereas many 4N nuclei in category 8 had dumbbell or irregular shapes and consequently high PAR values, evidently from failure in cytokinesis.

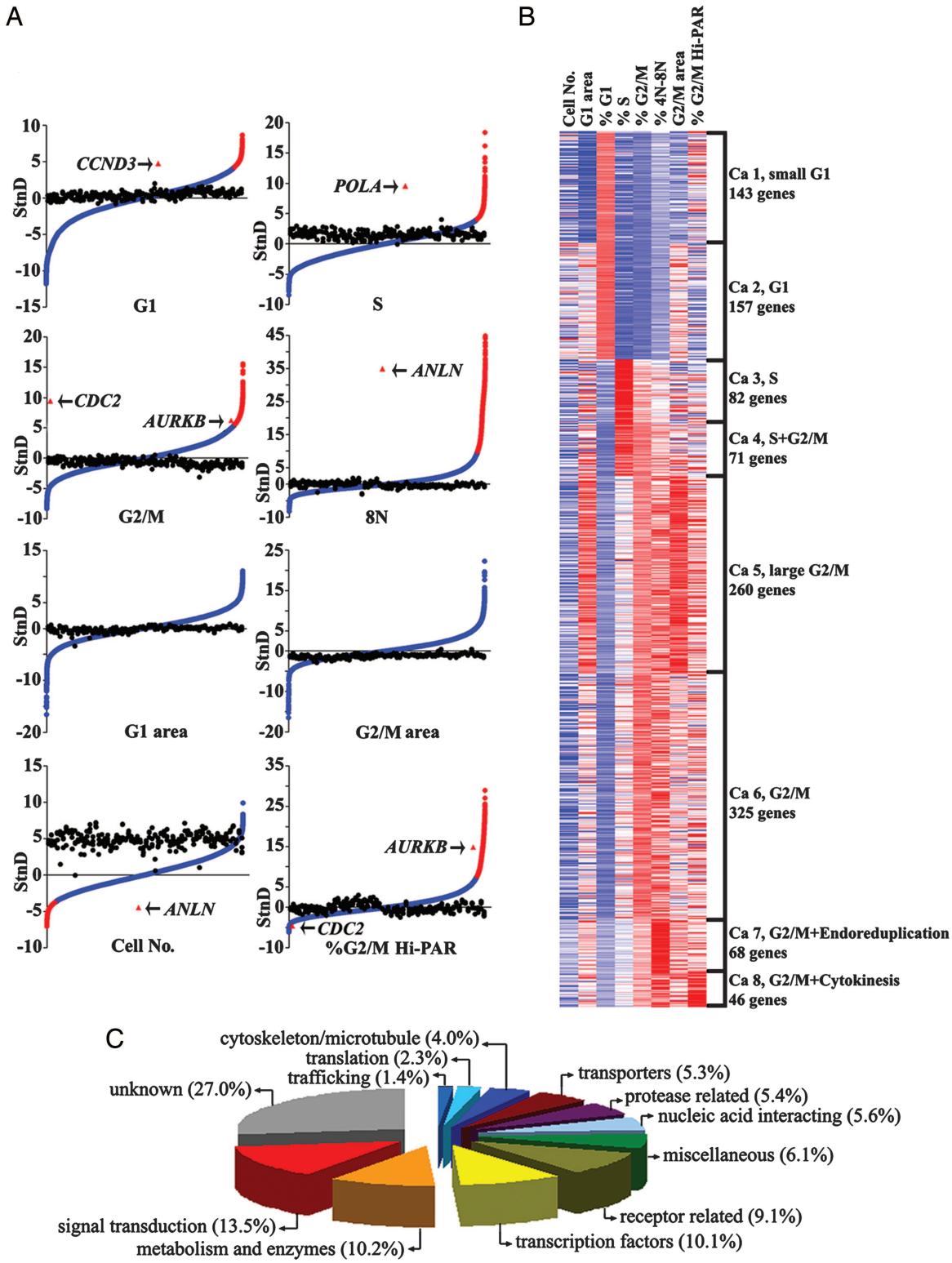

Fig. 2. Quantitative measurements and functional classification of genes from the genome-wide RNAi screen for human cell-cycle regulators. (*A*) Scores for the eight descriptors plotted as rank vs. standard deviations (StnD). The top 1,000 scoring genes are shown as red circles, GL3 controls (targeting luciferase) as black circles, selected known genes as red triangles, and all other genes as blue circles. (*B*) Cluster analysis of the normalized scores for the eight descriptors of each cell-cycle gene (*x* axis) resulted in eight distinct phenotypic categories (Ca, *y* axis). Normalized scores of $\geq +3$ are red, ≤ -3 blue, and 0 white. (*C*) Pie chart showing the putative biological processes, based on GO and Interpro annotations, of cell-cycle regulators.

Whereas down-regulation of the majority of the genes in these categories likely results in cell-cycle arrest in the given phase, some genes may have functions in parts of the cell cycle distinct from the phase that shows increased population. Depletion of known inhibitors of G_1 progression like p27 kip1 also increased the percentage of cells with 4N DNA content, likely by reducing

the time required to enter S phase (17). In another example, down-regulation of genes important for DNA synthesis like the 40-kDa subunit of the DNA synthesis accessory protein replication factor C (*RFC2*, category 6) and replication protein A1 (category 4) caused a G_2/M arrest after transfection with two distinct siRNAs. Indeed, in fission yeast, many S phase mutants with apparently replicated DNA undergo cell-cycle arrest, unable to complete mitosis (18). This arrest reflects activation of a checkpoint and indicates that replication is actually incomplete or the DNA is damaged.

Classification of Cell-Cycle Genes by Protein Function. When the identified proteins were classified into distinct cellular processes according to their Gene Ontology (GO) and Interpro (European Bioinformatics Institute) annotations, the largest class was genes with no known or predicted functions (27%) (Fig. 2*C* and Table 4, which is published as supporting information on the PNAS web site). The second largest category was signal transduction genes, which include protein kinases, phosphatases, second messenger-related proteins, and their modulators. The prevalence of kinases is not surprising because cell-cycle progression is a phosphorylation-driven process, and well studied kinases such as *CDK1* and *PLK1* were identified. Down-regulation of Ser/Thr phosphatases also resulted in G_2/M arrest. Protein phosphatase 1 (PP1) loss-of-function studies in yeast, *Drosophila*, and mammalian cells suggest that PP1 has several substrates during mitosis and cytokinesis (19). In our screen, depletion of the PP1 catalytic subunit *PPP1CB* led to an increase in the population of G_2/M cells. PP1 is reported to have >50 regulatory subunits, and, whereas many PP1-interacting proteins have been implicated in diverse cellular functions, the full complement of cell-cycle-related subunits is not known. RNAi of the putative PP1 regulator *PPP1R3F* resulted in G_2/M arrest, as did down-regulation of the protein kinase C-potentiated PP1 inhibitor *PPP1R14A*. In addition, depletion of *PPP1R9A*, a PP1-interacting protein associated with the actin cytoskeleton, caused a G_2/M arrest with increased endoreplication.

In addition to regulation by phosphorylation, the activities of many cell-cycle proteins are controlled by periodic ubiquitin/proteasome-mediated proteolysis. We have identified a number of ring finger and F-box proteins, including *SKP2* and *FBXO5* (Emi). Some of the novel F-box proteins identified (*FBXL2*, *FBXL10*, *FBXL16*) have an N-terminal F-box and C-terminal leucine-rich and/or jumonji protein interaction domains, a characteristic feature observed in F-box proteins that form the substrate recognition subunit of SKP1-cullin-F-box ubiquitin ligase complex (SCF).

Genome-wide analysis of genes required for cell-cycle progression has also identified classes of proteins not previously investigated for function in specific phases. Surprisingly, we have identified a large number of receptors and their modulators (53 genes), metabolism-related genes (60 genes), and translation-related genes (11 genes) that seem essential for G_2/M progression (categories 5 and 6). Although there is divergence in the specific homologs in each functional category, similar patterns have also been observed in *Drosophila* (Table 5, which is published as supporting information on the PNAS web site) (9, 20) and other human cell types (12). For example, the importance of receptor-mediated signaling in G_2/M progression is underscored by the finding that down-regulation of the receptor tyrosine kinase Pvr (*Drosophila* homolog of human VEGFR) and one of its ligands (Pvf2) increases the G_2/M population in *Drosophila* S2 cells (9, 20). Thus, whereas extracellular signals, nutritional status, and translational control are typically thought to regulate G_0-G_1 or G_1-S transitions, our results suggest that these processes contribute to as yet uncharacterized G_2/M transitions. In addition, genes from each of the other functional classes were also found to be important for virtually all phases of cell-cycle progression (Table 4). In particular, a broad range of ion channels and solute carriers were found to regulate multiple stages of the cell cycle (65 transporters and related genes), consistent with a large body of evidence suggesting roles for these gene families in cell-cycle progression and cell proliferation (21).

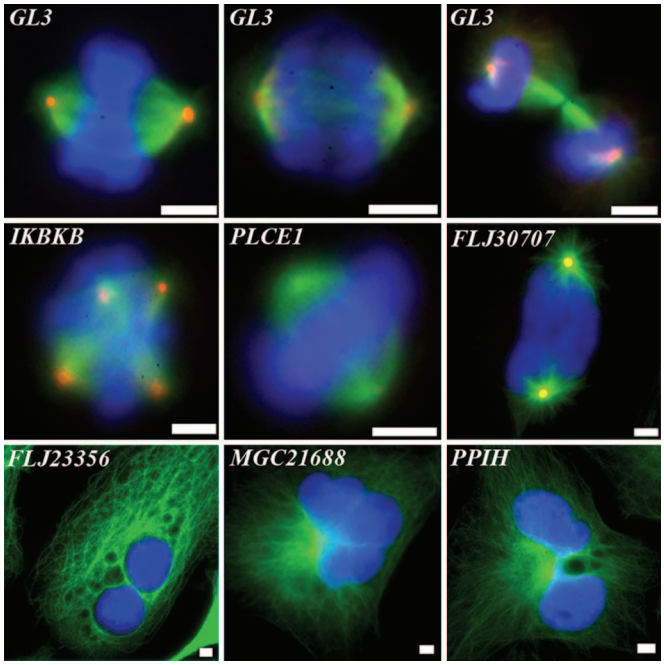

Fig. 3. Examples of mitotic and cytokinetic defects after RNAi of indicated genes. U2OS cells were stained with anti-γ-tubulin antibody (red), anti-α-tubulin (green), and DAPI (blue). (Scale bars: 5 μm.)

Knowledge-Based Network Analysis of Cell-Cycle Genes. To develop phase-specific networks that characterize the relationships between these genes, we mapped the genes to a comprehensive knowledge-based database (22). Analysis of G_1 genes identified receptor tyrosine kinase (*FGFR4*, *NTRK3*), ras-mediated (*RASGEF1B*, *IQGAP1*) and integrin signaling components (*ITGA5*, *ITGA6*, *ITGA8*, *ITGB5*) that lead to activation of CDK4/6-cyclin D/pRB/E2F pathway (23) (Fig. 7, which is published as supporting information on the PNAS web site). Analysis of S phase networks identified enzymes involved in purine and pyrimidine metabolism that are essential for DNA synthesis, as well as several DNA polymerases (Fig. 7). We identified *HSPC037* as an S phase gene, the human ortholog of yeast Psf2, which forms part of the recently identified GINS complex in budding yeast and participates in the initiation of replication (24). We also identified several mRNA splicing and processing genes that increase S phase populations (categories 3 and 4), including *U2AF2*, *SLBP*, *LSM8*, *RNPS1*, and the hypothetical protein HSPC148, a homolog of the *S. pombe* Cwf15 protein and component of the spliceosome. Interestingly, an earlier cell division screen using endoribonuclease RNase III-prepared siRNA (esiRNA) identified seven splice factors involved in mitotic arrest (26), including *SNRPB*, which was also found in our study as a G_2/M gene. Analysis of the G_2/M genes identified known genes, including downstream targets of CDC2-cyclin B (Fig. 7) that are involved in key mitotic processes like Golgi fragmentation (*GORASP1*) (27), APC activation (*FZR1*/*CDH1*) (28), and chromosomal passenger complex formation (29) [*BIRC5*/survivin, aurora-B, incenp, and borealin/dasra-B (30)]. Depletion of a number of novel genes caused similar

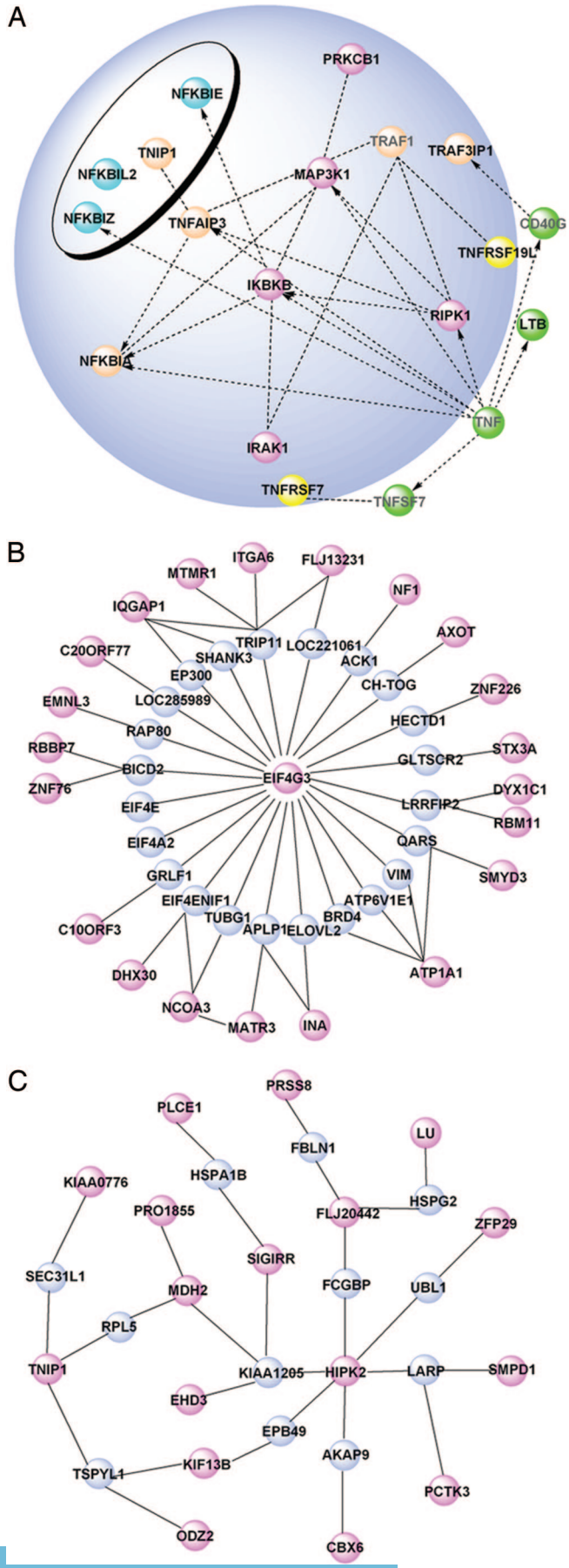

cytokinetic defects, including *FLJ23356* (an inactive predicted kinase), *MGC21688*, and *PPIH* (Fig. 3).

Our network analyses also identified at least 15 components of TNF/NF-κB signaling pathway as G_2/M genes (Figs. 4*A* and 7). TNF signaling plays a critical role in diverse cellular events, including cell proliferation, differentiation, and apoptosis. Whereas NF-κB signaling has previously been implicated in G_1-S progression (31), and depletion of the pathway kinases RIPK1 and IRAK1 have recently been found to increase mitotic index (12), little is known about this pathway's role in G_2/M phase. Depletion of *IKK-β* (*IKBKB*) by two independent siRNAs showed G_2/M arrest (Table 3) and caused multiple centrosomes (Fig. 3). These results suggest that IKBKB has pleiotropic effects in cell-cycle regulation and that many other TNF signaling genes also play unexpected roles in G_2/M progression.

Mapping of Cell-Cycle Genes onto a Protein–Protein Interaction Network. To gain insights into the function of poorly annotated genes and develop physical and functional maps (4, 9) for each phase of the cell cycle, we interrogated an extensive human yeast-two-hybrid protein interaction network with the cell-cycle genes described here. The resulting phase-specific protein interaction networks involving 89 G_1 genes in 498 interactions, 47 S phase genes in 207 interactions and 323 G_2/M genes in 2,218 interactions (Fig. 8, which is published as supporting information on the PNAS web site) (information on the protein–protein interactions is available at www.prolexys.com/data/Mukherji_et_al_2006_tables.xls) had significantly higher internal connectivity compared with randomized networks from the database (Fig. 8). Within these large networks, clusters of genes with common phenotypes can be identified. For example, a G_1 subnetwork of genes with small nuclei centers on *EIF4G3*, a large scaffolding protein that is critical for translation initiation (Fig. 4*B*). Three *EIF4G3* primary interactors were EIF family members, and 15/20 G_1 secondary interactors were $>1.7\ \sigma$ smaller than average, indicating that most genes in this subcluster were similar in phenotype.

Another example of phenotypic clustering included G_2/M genes with high phosphohistone content, which are likely to play functional roles during mitosis. Out of 34 phosphohistone-positive genes, 17 genes were found in one subcluster that were connected with 29 interactions (Fig. 4*C*). Three members of this subnetwork are associated with TNF signaling (*TNIP1*, *PRO1855*, and *SIGIRR*). This subnetwork also consisted of several signaling proteins, including kinases (*HIPK2* and *PCTK3*), a protein phosphatase (*DUSP23*/*FLJ20442*), and second messenger synthesizing enzymes (*PLCE1* and *SMPD1*). *PLCE1*, a ras-activated phospholipase, is responsive to extracellular signaling and confers resistance to chemical carcinogenesis when inactivated in the mouse (32). Immunocytochemical analysis of mitotic cells after *PLCE1* down-regulation showed a loss of γ-tubulin at the spindle poles during metaphase (Fig. 3). Further, several genes in the subnetwork are associated with the cytoskeleton, including EHD3, an eps15 homology domain containing protein. Overexpression of EHD3 resulted in several binucleated cells (data not shown) and localized to large tubular structures, in agreement with an earlier study (33).

Relevance of Screen Results to Cancer. In addition to cell-cycle analysis, our high-content imaging method allowed us to monitor

Fig. 4. Subnetworks showing protein associations among cell-cycle regulators. (*A*) G_2/M genes involved in TNF signaling. Gene symbols in black are identified in this study. Node colors represent transcription regulators (blue), enzymes (red), receptors (yellow), growth factors (green), and other proteins (brown). (*B*) G_1 proteins showing the clustering of translation components and genes giving rise to the small nucleus G_1 phenotype. Shown are cell-cycle regulators (red) and genes with no phenotype (blue). (*C*) Mitotic proteins within the G_2/M network. Color codes are the same as in *B*.

cell proliferation and cell size (Table 6, which is published as supporting information on the PNAS web site). Inappropriate control of cell cycle and proliferation are important factors in tumorigenesis. Interestingly, among the identified cell-cycle genes, >20% with an Online Mendelian Inheritance in Man (OMIM) entry are cancer-associated, and 130 genes were found to have elevated mRNA levels in primary tumor samples, compared with normal tissue as assessed by microarray experiments (Table 7, which is published as supporting information on the PNAS web site). Thus, our loss-of-function study has identified a number of genes that could be targeted with small molecules as anti-cancer agents.

In summary, we have targeted >95% of currently known or predicted human genes with siRNAs to determine their quantitative effects in the regulation of cell cycle, cell size, and cell proliferation. These analyses resulted in the identification of numerous known genes as well as novel functions for known and predicted genes. Our estimate that ≈5% of genes regulate cell-cycle progression is likely a conservative one because our screening criteria were stringent. Nonetheless, the integrative approach described here serves as the basis for systems-level model building (34), which suggests testable hypotheses that can be refined with further experimentation.

Materials and Methods

Detailed materials and methods are presented in *Supporting Materials and Methods*, which is published as supporting information on the PNAS web site.

A genome-wide library of 48,746 siRNAs targeting 24,373 genes was designed by using an artificial neural network (10). An additional library consisting of 10,000 siRNAs targeting 5,000 selected genes from the human genome was designed by using a previously reported algorithm (35). One microliter of siRNA targeting a particular human gene was spotted into each well of 384-well black clear bottom plates. The siRNAs were transfected into U2OS cells (2,000 cells per well) in culture media (12.5 nM siRNAs final concentration) and grown for 3 days. The cells were washed, fixed in 4% paraformaldehyde, and imaged on an automated inverted fluorescence microscope. Twenty images were collected per well by using filters appropriate for DAPI fluorophore and processed with CYTOSHOP software. Typical densities for negative control transfections using GL3 siRNA (a sequence-targeting firefly luciferase GL3 that does not cross-hybridize with any human gene) were ≈6000 cells per well. For each plate, histograms of number of objects per nuclei vs. total nuclear fluorescence for GL3 siRNA-transfected wells were plotted, and the boundaries for G_1, S, G_2/M, and 8N phases of the cell cycle were determined. Processed wells were gated for each phase of the cell cycle, and percentages of cells in each phase were calculated for every well.

We thank Christina Kohler, Paul DeJesus, Christopher Trussell, Amit Phansalkar, and Anthony Marelli for technical assistance and Prof. Wei Jiang, Prof. Steven Reed, Andrew Su, Leif Dehmelt, and John Walker for helpful discussions. This work was supported by funding from the Novartis Research Foundation. M.M. is a Skaggs Postdoctoral Fellow. This is manuscript 17927-CH of The Scripps Research Institute.

1. Nurse P, Masui Y, Hartwell L (1998) *Nat Med* 4:1103–1106.
2. Sonnichsen B, Koski LB, Walsh A, Marschall P, Neumann B, Brehm M, Alleaume AM, Artelt J, Bettencourt P, Cassin E, *et al.* (2005) *Nature* 434:462–469.
3. Boutros M, Kiger AA, Armknecht S, Kerr K, Hild M, Koch B, Haas SA, Consortium HF, Paro R, Perrimon N (2004) *Science* 303:832–835.
4. Kim JK, Gabel HW, Kamath RS, Tewari M, Pasquinelli A, Rual JF, Kennedy S, Dybbs M, Bertin N, Kaplan JM, *et al.* (2005) *Science* 308:1164–1167.
5. Philips JA, Rubin EJ, Perrimon N (2005) *Science* 309:1251–1253.
6. Agaisse H, Burrack LS, Philips JA, Rubin EJ, Perrimon N, Higgins DE (2005) *Science* 309:1248–1251.
7. Muller P, Kuttenkeuler D, Gesellchen V, Zeidler MP, Boutros M (2005) *Nature* 436:871–875.
8. DasGupta R, Kaykas A, Moon RT, Perrimon N (2005) *Science* 308:826–833.
9. Bjorklund M, Taipale M, Varjosalo M, Saharinen J, Lahdenpera J, Taipale J (2006) *Nature* 439:1009–1013.
10. Huesken D, Lange J, Mickanin C, Weiler J, Asselbergs F, Warner J, Meloon B, Engel S, Rosenberg A, Cohen D, *et al.* (2005) *Nat Biotechnol* 23:995–1001.
11. Silva JM, Li MZ, Chang K, Ge W, Golding MC, Rickles RJ, Siolas D, Hu G, Paddison PJ, Schlabach MR, *et al.* (2005) *Nat Genet* 37:1281–1288.
12. Moffat J, Grueneberg DA, Yang X, Kim SY, Kloepfer AM, Hinkle G, Piqani B, Eisenhaure TM, Luo B, Grenier JK, *et al.* (2006) *Cell* 124:1283–1298.
13. Perlman ZE, Slack MD, Feng Y, Mitchison TJ, Wu LF, Altschuler SJ (2004) *Science* 306:1194–1198.
14. Whitfield ML, Sherlock G, Saldanha AJ, Murray JI, Ball CA, Alexander KE, Matese JC, Perou CM, Hurt MM, Brown PO, Botstein D (2002) *Mol Biol Cell* 13:1977–2000.
15. de Lichtenberg U, Jensen LJ, Brunak S, Bork P (2005) *Science* 307:724–727.
16. Rustici G, Mata J, Kivinen K, Lio P, Penkett CJ, Burns G, Hayles J, Brazma A, Nurse P, Bahler J (2004) *Nat Genet* 36:809–817.
17. Li WQ, Jiang Q, Aleem E, Kaldis P, Khaled AR, Durum SK (2006) *J Exp Med* 203:573–582.
18. Rhind N, Russell P (1998) *Curr Opin Cell Biol* 10:749–758.
19. Ceulemans H, Bollen M (2004) *Physiol Rev* 84:1–39.
20. Bettencourt-Dias M, Giet R, Sinka R, Mazumdar A, Lock WG, Balloux F, Zafiropoulos PJ, Yamaguchi S, Winter S, Carthew RW, *et al.* (2004) *Nature* 432:980–987.
21. Kunzelmann K (2005) *J Membr Biol* 205:159–173.
22. Calvano SE, Xiao W, Richards DR, Felciano RM, Baker HV, Cho RJ, Chen RO, Brownstein BH, Cobb JP, Tschoeke SK, *et al.* (2005) *Nature* 437:1032–1037.
23. Schwartz MA, Assoian RK (2001) *J Cell Sci* 114:2553–2560.
24. Takayama Y, Kamimura Y, Okawa M, Muramatsu S, Sugino A, Araki H (2003) *Genes Dev* 17:1153–1165.
25. Ohi MD, Link AJ, Ren L, Jennings JL, McDonald WH, Gould KL (2002) *Mol Cell Biol* 22:2011–2024.
26. Kittler R, Putz G, Pelletier L, Poser I, Heninger AK, Drechsel D, Fischer S, Konstantinova I, Habermann B, Grabner H, *et al.* (2004) *Nature* 432:1036–1040.
27. Sutterlin C, Polishchuk R, Pecot M, Malhotra V (2005) *Mol Biol Cell* 16:3211–3222.
28. Bembenek J, Yu H (2001) *J Biol Chem* 276:48237–48242.
29. O'Connor DS, Grossman D, Plescia J, Li F, Zhang H, Villa A, Tognin S, Marchisio PC, Altieri DC (2000) *Proc Natl Acad Sci USA* 97:13103–13107.
30. Sampath SC, Ohi R, Leismann O, Salic A, Pozniakovski A, Funabiki H (2004) *Cell* 118:187–202.
31. Aggarwal BB (2004) *Cancer Cell* 6:203–208.
32. Bai Y, Edamatsu H, Maeda S, Saito H, Suzuki N, Satoh T, Kataoka T (2004) *Cancer Res* 64:8808–8810.
33. Galperin E, Benjamin S, Rapaport D, Rotem-Yehudar R, Tolchinsky S, Horowitz M (2002) *Traffic* 3:575–589.
34. Gunsalus KC, Ge H, Schetter AJ, Goldberg DS, Han JD, Hao T, Berriz GF, Bertin N, Huang J, Chuang LS, *et al.* (2005) *Nature* 436:861–865.
35. Aza-Blanc P, Cooper CL, Wagner K, Batalov S, Deveraux QL, Cooke MP (2003) *Mol Cell* 12:627–637.